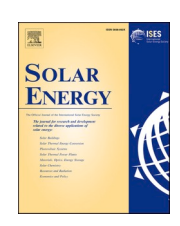
ELSEVIER

#### Contents lists available at ScienceDirect

#### Solar Energy

journal homepage: www.elsevier.com/locate/solener





# Electroluminescence inspections of PV modules and strings by a self-powering configuration in daylight mode

L.A. Carpintero <sup>a,b,\*</sup> , C. Terrados <sup>a,c</sup>, D. González-Francés <sup>a</sup>, K.P. Sulca <sup>a</sup>, V. Alonso <sup>d</sup>, M.A. González <sup>a</sup>, O. Martínez <sup>a</sup>

- a GdS-Optronlab Group, Dpto. Física de la Materia Condensada, Universidad de Valladolid, Edificio LUCIA, Paseo de Belén 19, 47011 Valladolid, Spain
- <sup>b</sup> Cobra Instalaciones y Servicios, S.A. Calle Cardenal Marcelo Spinola, 10, 28016 Madrid, Spain
- c Solar and Wind Feasibility Technologies (SWIFT), Escuela Politécnica Superior, Universidad de Burgos, Avda. Cantabria s/n, 09006 Burgos, Spain
- d GdS-Optronlab Group, Dpto. Física Aplicada, Universidad de Valladolid, Facultad de Ciencias, Paseo de Belén 7, 47011 Valladolid, Spain

#### ARTICLEINFO

# Keywords: Solar cell defects Daylight electroluminescence dEL imaging PV module diagnostics On-site inspection Self-powering

#### ABSTRACT

Electroluminescence (EL) imaging is a widely used tool for identifying defects in the solar cells of photovoltaic (PV) modules. Traditional EL inspections require dark conditions and module disassembly, making them costly and logistically challenging. Daylight Electroluminescence (dEL) has emerged as a cost-effective alternative, enabling on-site inspections under any irradiance conditions without module dismounting and thereby reducing costs. However, EL inspections require current injection, necessitating an external power source. Solutions like bidirectional inverters have been proposed to address this challenge. This study proposes a novel self-powered dEL methodology that uses other PV strings in the plant to supply the necessary current. The method employs a switching procedure to filter ambient light and allows entire string inspection without dismounting modules or using external power. Field tests across various irradiance conditions show that the resulting images are comparable to those obtained in controlled darkroom environments, validating the method's effectiveness and operational advantages.

#### 1. Introduction

Following the 2030 Agenda for Sustainable Development [1,2] and the Paris Agreement, renewable energy has gained momentum as an alternative to fossil fuels [3].

Photovoltaic (PV) energy, in particular, stands out for its modularity, ease of assembly, and low maintenance costs. Technological advances and reduced production costs have further lowered the Levelized Cost of Energy (LCOE) for PV, making it one of the most economically viable energy sources in many regions [4]. The significant rise in PV installations, with solar PV making up 46 % of global renewable capacity by the end of 2024 [5], necessitates strict verification protocols. Adherence to IEC standards, such as IEC 62446 for grid-connected systems [6], is crucial for ensuring system efficiency and reliability. This growth also highlights the need for cost-effective inspections to maintain profitability.

Essential inspections include evaluating solar modules for defects throughout their lifecycle to ensure proper functioning [7–9].

Techniques like I-V curve analysis, visual inspections, infrared thermography (IRT), and electroluminescence (EL) imaging are widely used by operation and maintenance (O&M) teams [10,11]. Electroluminescence imaging is the most precise for detecting micro-cracks, broken interconnections, and shunts [12]. Its ability to assess solar cell quality makes it critical for preventing module degradation and optimizing PV plant performance.

Traditional EL inspections rely on silicon-based (Si) cameras in dark conditions [13], module disassembly and transport to darkrooms or mobile labs [14], making it time-consuming and costly. These processes are often limited to small samples, risking undetected defects in larger installations. Furthermore, disassembly and transport can inadvertently damage modules, adding to inspection challenges. Alternative methods, such as night-time EL or using covers for darkness, or PL imaging using lamp/LED light sources for excitation [14–20] still require external power sources, often involving bulky equipment like generators, which are difficult to transport and operate on uneven terrain.

Within PV diagnostics, daylight EL (dEL) has emerged as a promising

E-mail address: lacarpintero@grupocobra.com (L.A. Carpintero).

https://doi.org/10.1016/j.solener.2025.113913

Received 20 February 2025; Received in revised form 5 August 2025; Accepted 21 August 2025 Available online 27 August 2025

0038-092X/© 2025 The Author(s). Published by Elsevier Ltd on behalf of International Solar Energy Society. This is an open access article under the CC BY license (http://creativecommons.org/licenses/by/4.0/).

<sup>\*</sup> Corresponding author at: GdS-Optronlab Group, Dpto. Física de la Materia Condensada, Universidad de Valladolid, Edificio LUCIA, Paseo de Belén 19, 47011 Valladolid, Spain.

solution [21–25], enabling EL inspections during daytime with high-quantum-efficiency (QE) infrared cameras (e. g., InGaAs) and ambient light filtration. When applied to PV modules, dEL eliminates the need for disassembly, allowing inspections under any irradiance conditions. However, it still requires current injection, often necessitating power sources like generators or bidirectional inverters, which present logistical and economic challenges. Daylight PL (dPL) has also been developed parallel to dEL and has the advantage of not needing a power source for excitation, as it uses the sun as a light excitation source [23,26,27], needing also ambient light filtration. Various approaches have been used to obtain the dPL image by switching the panels between two states for which purpose electrical or optical switching have been developed [28–35]. While dPL provides useful information about defects in solar cells without the need for a power source, dEL imaging provides additional information [36].

This work introduces a new self-powering method for dEL inspections using other PV strings to supply current. This minimizes external power needs, reducing costs and environmental impact. Field tests under real unlight demonstrate its effectiveness, achieving results comparable to traditional methods while enhancing inspection efficiency and reliability.

#### 2. Methodology

We present a new method for dEL inspection of entire strings, using a self-powering configuration that injects current without requiring an external supply. It leverages the typical field setup of parallel-connected strings and works without blocking diodes or bypassing them.

The core concept is to use modules from the photovoltaic plant itself as a power source to inject the necessary current into the string or group of modules for dEL testing. Inspection takes place during daylight hours, where the sunlight irradiance on the plant's modules generates the current needed to bias the modules under analysis.

The PV modules located in a PV plant usually display the same characteristics and are grouped into sets with the same number of modules connected in series that are called strings. These sets are grouped in parallel in a bus cable that reaches an element (generally second level boxes) from where a power line is routed to the inverter.

The proposed methodology is based on the assumption that, for any configuration of a solar PV plant, it is always possible to isolate sets of strings from the production and to ensure that one of these –labelled as string B– injects current into another string –labelled as string A– provided that string B has a greater number of modules in series than

string A; Fig. 1. That is, if string B has s modules in series, string A must have s-1 modules in series or less, s-n.

However, due to the characteristic of the I-V curve of a PV module or a set of them in series, a single string B connected in parallel with a string A is not always capable of injecting the current required to obtain EL images if the voltage difference between the set of modules in series A and string B—caused by the difference in the number of modules in string A and string B— is not sufficient. In other words, if string A has only one or two fewer modules in series than string B, the operating point to be set on string A may not provide much current in relation to the short circuit current ( $I_{sc}$ ) of the photovoltaic modules involved. To achieve the appropriate operating point, several strings B (with s PV modules in series each one) can therefore be associated by connecting them in parallel.

To help inject the current necessary to obtain the EL measurements, several strings B can be arranged in parallel with a string A. With p denoting the number of strings B (each with s modules) placed in parallel with string A, with s-n modules, there are therefore s times p modules injecting current into the s-n modules of string A; Fig. 1.

More complex combinations of modules associated in series and parallel are equally possible. To inject current into the set to be measured (which may be several strings A), the total number of modules that generate current (that is, the modules that are part of the set of strings B) must have the necessary characteristics (higher open-circuit voltage and sufficiently high total power) so that the current injected into strings A is in the appropriate range, which can be defined in the range 80 %–100 % of the short circuit current ( $I_{sc}$ ) of the set of strings A.

In a very common situation in real plants, all the strings will have s modules in series, such that string A is one of them, to which n modules have been disconnected so that a set of strings B, in parallel with it, is able to inject current into it. With any other configuration of modules, it would be equally possible to inject current from one string to another, provided that the string under study has a lower open circuit voltage than the string(s) powering it.

The modules to be analysed form part of the string or strings under study, which will be powered by the rest of the strings connected in parallel to the same second level box (commonly called combiner box, CB). These strings will be responsible for injecting the current necessary to bias the modules to be analysed.

For the practical implementation of the inspection, it is therefore necessary to first form a set of strings of PV modules that will act as a power source (string or strings that inject current –Strings that Power–labelled  $S_P$ ) and to define a string of PV modules in which the dEL

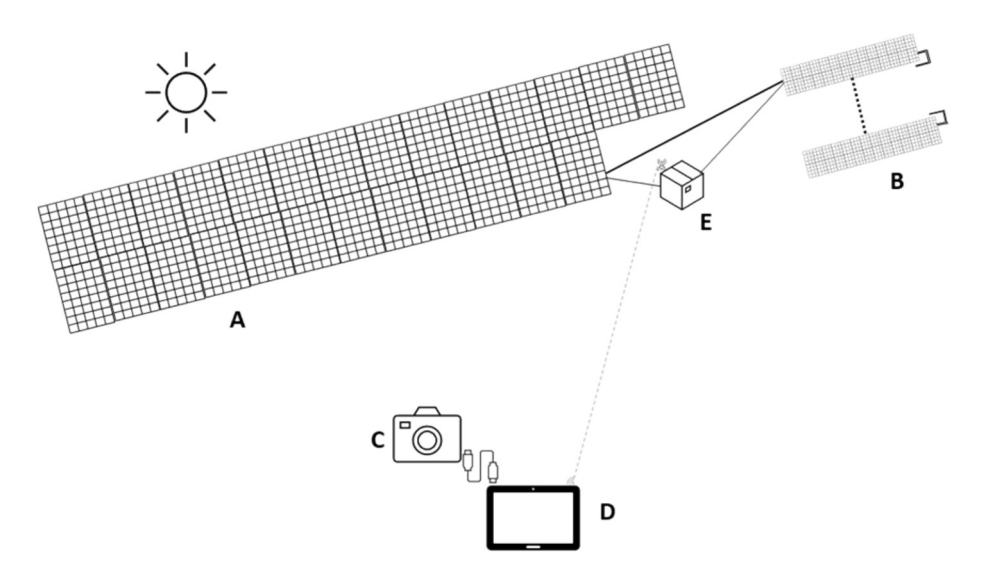


Fig. 1. Schematic diagram of the dEL method by a self-powering configuration. A = string under study; B = strings used to inject current; C = InGaAs camera; D = unit control; E = electronic switching device.

measurement will be carried out (String to be Measured –labelled S<sub>M</sub>). In addition, a device called an electronic switching device (ESD) is connected between the S<sub>P</sub> and S<sub>M</sub> strings. This device, developed by our research group, acts as a switch that cuts the current between the two sets of strings (S<sub>P</sub> and S<sub>M</sub>), obtaining two states on S<sub>M</sub>: ON state, where the current circulates from S<sub>P</sub> to S<sub>M</sub> through the ESD and thus generates the electroluminescence of the string S<sub>M</sub>, and OFF state, where the ESD works to prevent current from circulating, and no electroluminescence is emitted. The electronic switching device is thus connected in series between S<sub>P</sub> and S<sub>M</sub>. As indicated previously, in a PV plant with identical strings of s modules,  $S_P$  can be made up of s times p PV modules, with p being the number of strings connected in parallel in the set, and S<sub>M</sub> being comprised of s-n PV modules. The most suitable number n is selected in order to have an adequate value of the current that circulates from set SP to S<sub>M</sub>. By connecting or disconnecting PV modules from string S<sub>M</sub>, the optimal number n is obtained when the current is similar to that of the  $I_{sc}$ value of string S<sub>M</sub>. A range of currents between 0.8 I<sub>sc</sub> and ·I<sub>sc</sub> could be considered good enough for the dEL measurements. Having fixed strings  $S_P$  and  $S_M$  with the number n to have an optimum current, dEL measurement consists of taking a number of images with the InGaAs camera, alternatively electrically connecting (ON state) and disconnecting (OFF state) the set S<sub>P</sub> to S<sub>M</sub>, which is performed by means of the switching and control device. As explained in detail in Ref. [23], our system involves synchronised switching between current injection (via ESD) and exposure of the InGaAs camera. The ESD is typically switched at a frequency of between 0.1 and 1 Hz, synchronised via a control unit to the camera exposure sequence. The final dEL image is obtained by the sum of the differences I<sub>ON</sub>-I<sub>OFF</sub> [23]. Currently, field technicians manually adjust the number of modules to disconnect (n) based on prior calculations and typical irradiance conditions.

Using this procedure and powering sequence, it is possible to quickly, easily, and safely bias the desired modules on-site, allowing EL tests to be carried out in daylight mode (dEL). To ensure the safety of maintenance personnel, it is necessary to implement comprehensive energy source isolation. The first step is to open the combiner or string box unit (open circuit breaker). Once the combiner box has been accessed, the power supply to the inverter has been cut off to create the necessary separation between the positive and negative conductors. This isolation sequence enables technical staff to disconnect modules without risking an arc flash, thereby maintaining safe operational parameters throughout the maintenance procedure. This begins with opening the circuit breaker in the combiner/string box to cut power to the inverter. Next, clamp meter readings verify no significant current imbalances before opening the MC4 connector. Finally, the string's positive terminal is connected to the ESD device's positive, and the ESD's negative to the module's positive. This procedure adheres to safety guidelines for PV installations.

#### 3. Experimental set-up

To conduct dEL inspection of whole strings by means of the self-powering configuration, the set-up includes a camera with an InGaAs sensor (Hamamatsu C12741-03 model, with  $640\times512$  pixels, in our case), appropriate optical filters, ESD and control acquisition software (see Fig. 2). Two Kowa lenses (LM16HC-SW and LM8HC-SW with 16 and 8 mm focal length, respectively) were utilized with the camera. A SWIR bandpass filter –centred around 1160 nm with a bandwidth of 150 nm and a transmittance close to 90 %– is used.

Tests were carried out in different 50 MW PV plants located in Spain that were in commercial operation (real situations), using both c-Si and mc-Si monofacial half-cell technologies, on over 2,000 modules. Measurements were taken throughout the year under varying weather and sunlight conditions. The Irradiance ranged from 200-500 W/m² during the overcast November-December to  $\sim 1000~\text{W/m}^2$  in July-August. Temperatures varied from (4–6) °C in winter to (35–37) °C in summer.

The results shown here correspond to a 50 MW plant of c-Si modules,



Fig. 2. Set-up used for dEL inspections by the self-powering configuration.

PERC modules (435 W<sub>p</sub>,  $I_{SC} = 11.20$  A,  $V_{OC} = 49.4$  V, Module Efficiency = 19.7 %), with strings of 28 modules and with 12 strings per combiner box, and to a 50 MW plant of mc-Si modules (345 Wp,  $I_{SC} = 9.55$  A,  $V_{OC}$ = 46.3 V, Module Efficiency = 17.4 %), with strings of 30 modules and with 24 strings per combiner box. In both cases, the whole string (of 28 or 30 modules) consists of modules in two rows, mounted on tables with an automated mobile axis. Whole strings were inspected (except for the modules disconnected from them). Some measurements were performed on modules that were also inspected by electroluminescence using Si cameras under dark conditions in a laboratory (lab-EL), by disassembling them from the PV plant, sending them to the laboratory, and then reinstalling them. This module removal was predetermined for contracted lab-EL inspection in accordance with the facility's operation and maintenance program of the PV plants. In this way, it was possible to compare the two measurements and, in some cases, to compare the dEL images of modules obtained on-site before and after disassembly/reassembly for lab-EL inspection.

#### 4. Results and discussion

#### 4.1. Simulations

Prior to performing an experimental study of the capabilities of our self-powering method to carry out dEL inspections, numerical simulations were conducted using LTSPice to simulate the current injected on a string,  $S_M$ , which is powered by several strings in parallel,  $S_P$ , as in Fig. 3.

To simulate the injected current in the  $S_M$ , the simplest photovoltaic cell model—the single-diode model— was used [37,38] since it provides a sufficiently reliable estimate for the experimental design and safety assessment. This model consists of a current source representing the photogenerated current in the photovoltaic cell ( $I_{\rm ph}$ ), a parallel diode, a parallel (or shunt) resistance ( $R_{\rm sh}$ ), and a series resistance ( $R_{\rm s}$ ).

Additionally, the diode ideality factor (m, close to 1) and the temperature (*T*) are required. The parameters for single-diode model,

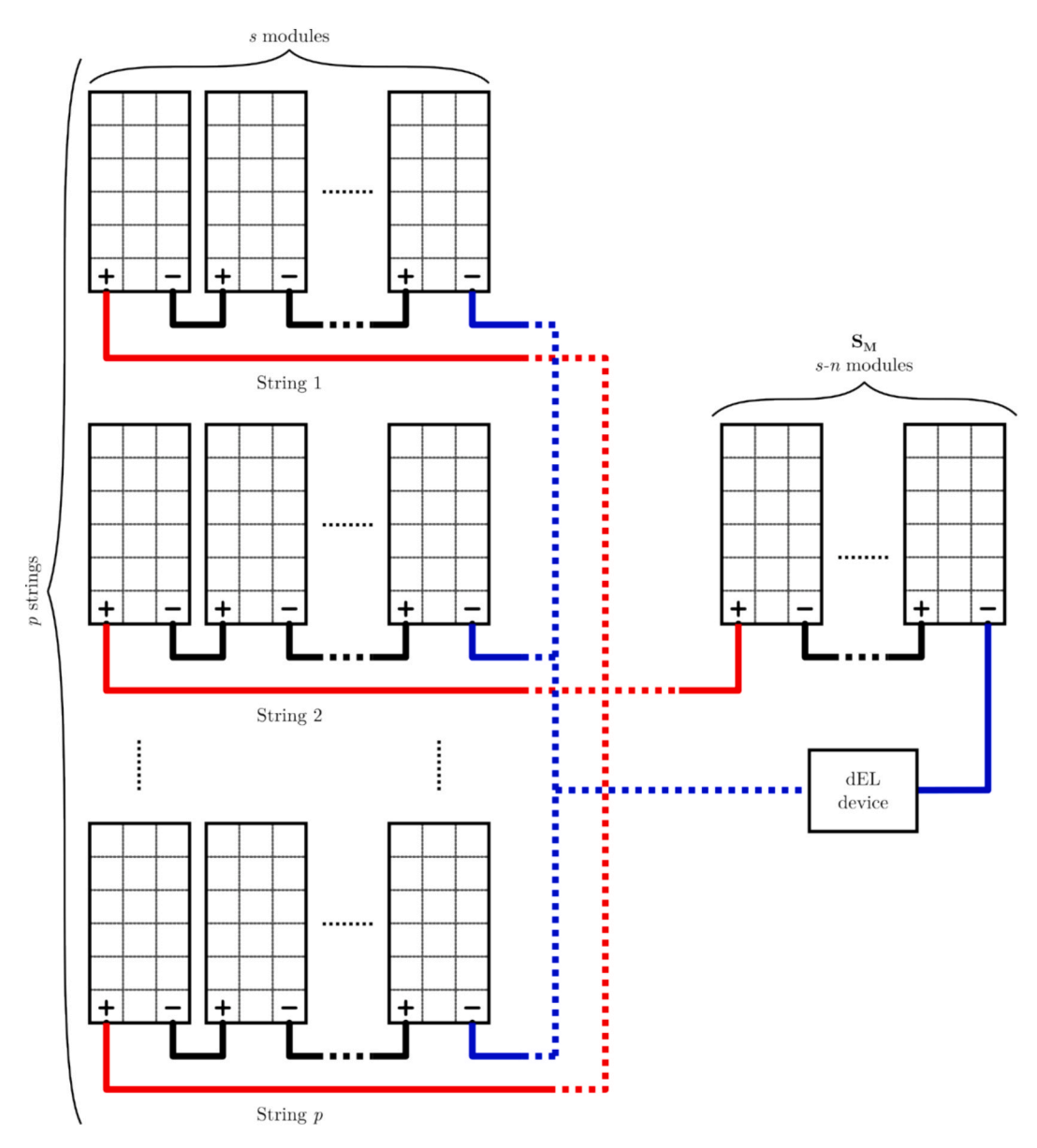


Fig. 3. Electrical wiring diagram of the configuration used to simulate the current injected on a string, S<sub>M</sub>, which is powered by several strings in parallel, S<sub>P</sub>.

including the photogenerated current ( $I_{ph}$ ), series resistance ( $R_s$ ), parallel resistance ( $R_p$ ) and ideality factor (m), were derived from the manufacturer's datasheet ( $I_{SC}$ ,  $V_{OC}$  and adjustment from IV-curve) of the specific modules installed at the real plant location where the dEL measurements were conducted. The temperature effect is taken into account by using the Temperature Coefficients of  $V_{OC}$  and  $I_{SC}$ .

In our simulations, each photovoltaic module consists of 72 solar cells in series (or 144 half-cells, with 72 half-cells in series, in parallel with another 72 half-cells in series, which can be modelled similarly as 72 full cells in series). As explained and shown in Fig. 3, the modules of the same string are in series which –ignoring the bypass diodes present in each module – converts a string into a series association of  $72 \cdot s$  solar cells. For example, in the case of 30 modules in series per string,  $72 \cdot 30 = 2160$  identical solar cell in series.

With this data, we can simulate the I-V curve of that string for specific irradiance and temperature based on the data contained in the manufacturer's module specification sheet (also considering the corresponding correction factors for open-circuit voltage and short-circuit current with temperature). We have p strings of these in parallel, which multiplies the current by p times, leaving the voltages unchanged. For

example, in the case of 23 strings in parallel, the *I-V* curve of these will be the same for voltages but multiplied by 23 for currents at each point.

For the  $S_M$ , we similarly have  $72 \cdot (s-n)$  solar cells in series. For example, in the case of a string of 30 modules in series from which we have removed three modules,  $72 \cdot (30-3) = 1944$  identical solar cells in series. For this reason, the *I-V* curve of the  $S_M$  has a lower open-circuit voltage than the strings with all modules.

Being in parallel with the rest of the strings, the equilibrium of the total system occurs at a point where the open-circuit voltage of the  $S_M$  is exceeded, such that the  $S_M$  becomes a load for the others and moves to the fourth quadrant of its I-V curve (emitting electroluminescence, EL). At that point, the other strings are injecting the same total current as the  $S_M$  is consuming, such that the point at which the voltages of the I-V curve of the other p strings in parallel and that of the I-V curve of the  $S_M$  are equal can be mathematically calculated. The current is the same magnitude but with the opposite sign.

Fig. 4 shows the simulation performed for the mc-Si PV plant, with 30 modules per string, with each module having 144 silicon cells. Twenty-four strings in parallel were considered, with 23 forming the  $S_P$  set, and with the other one being the  $S_M$  string. The effect of removing

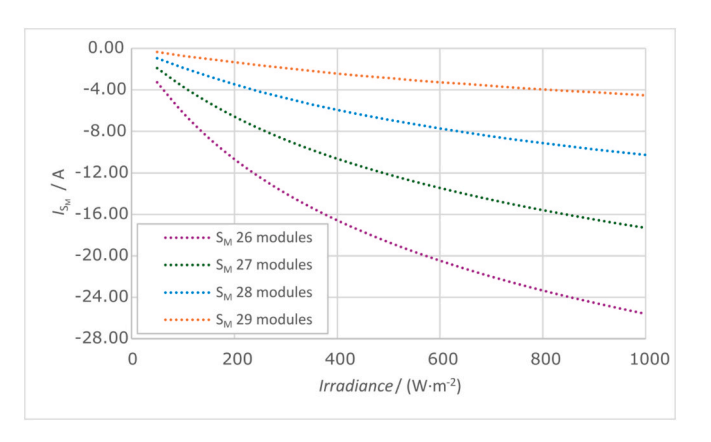


Fig. 4. Simulated current injected into  $S_M$  depending on the number of modules in the  $S_M$  vs irradiance at a cell temperature of 25 °C.  $S_P$  is formed by 23 strings of 30 modules. The effect of removing one, two, three, and four modules from the initial 30 modules ( $S_M$ ) is presented.

one, two, three, and four modules from the initial 30 modules was simulated, and was thus tested for an  $S_M$  string of 29, 28, 27, and 26 modules. Results are shown as a function of irradiance, with all of them calculated at a temperature of 25 °C.

As observed from the simulations, no more than two modules of the initial 30 modules that form the  $S_M$  string should be removed for this configuration in order to prevent the current surpassing the typical  $I_{SC}$  value of  $\sim\!10\!-\!11$  A. Furthermore, the number of modules to be removed depends on the sunlight irradiance conditions. As can be seen, removing two modules (string  $S_M$  of 28 modules) is quite a good option for medium to large irradiances.

The simulation reveals that disconnecting more panels within the  $S_{\rm M}$  string consistently increases the injected current, irrespective of irradiance. This allows for precise regulation of the injected current, preventing levels that could compromise module integrity and contribute to degradation or failure phenomena in PV modules.

Fig. 5 shows the simulation performed for the same mc-Si module PV plant case, but varying the temperature for a fixed number or modules on  $S_M$ . The effect of removing three modules from the initial 30 modules was simulated; in other words, for an  $S_M$  string of 27 modules. The simulation was performed for three different temperatures of the PV modules (25 °C, 50 °C, and 75 °C), and the results are shown as a function of the irradiance. Experimental results of the measured currents on the  $S_M$  string for this specific configuration have also been included.

From the values obtained, it can be seen that by only removing three

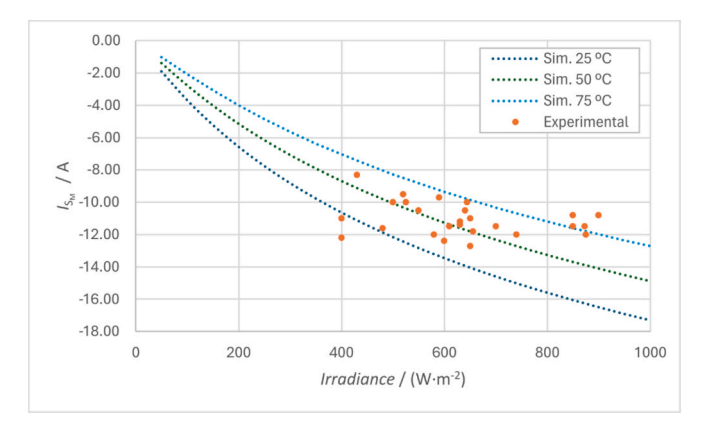


Fig. 5. Simulated  $I_{S_M}$  vs irradiance at three different temperatures.  $S_P$  is formed by 24 strings of 30 mc-Si modules. The effect of removing three modules from the initial 30 modules  $(S_M)$  is presented for three different temperatures of the PV modules. Experimental results –measured for this specific configuration– are also shown.

modules from the  $S_M$ , we are able to inject a current greater than 9 A, which is sufficient to be able to bias the  $S_M$ .

The variation in the measured values is due to cloud transients. It can be observed for instance that in some cases the current measured with radiation above  $900 \text{ W/m}^2$  (with clouds) is similar to those measured with sunlight irradiance of  $400 \text{ W/m}^2$ , at which time there was no cloud over the 24 strings and the sky was totally clear.

Based on this information, we find that on clear days and with high sunlight irradiance it is necessary to reduce the number of modules to be removed from the  $S_M$ , since otherwise, the short circuit current values would be exceeded.

#### 4.2. Experimental results

In order to show the capabilities of the self-powering configuration in the dEL mode, several measurements were performed in real 50 MW plants installed in Spain. The results presented here correspond to two PV plants, c-Si and mc-Si PV plants with the above-mentioned characteristics. Measurements were carried out varying the number n of disconnected modules in string  $S_M$ , with different irradiation conditions, and using different orientations of both the strings that injected the current  $(S_P)$  and that of the measured string  $(S_M)$ . Initially, dEL measurements were performed first for the whole string being measured and then for all individual modules of string  $S_M$  to obtain a higher-resolution dEL image of each PV module. For this purpose, the solar tracker was rotated  $180^\circ$  (on the rotation axis of the photovoltaic tracking assembly) in order to collect the dEL images of the modules of the bottom row at a closer distance, so that the modules are placed in the best positions to take the images as close as possible using a tripod fixed on the ground.

## 4.2.1. Whole strings imaging through dEL using the self-powering configuration

Fig. 6 shows the dEL images obtained by the self-powering configuration of whole strings in the mc-Si PV plant, where the number, n, of disconnected modules was 2 (Fig. 6(b)), 3 (Fig. 6(a and c)) or 4 (Fig. 6 (d)). As previously discussed, this number was selected in order to regulate the current injected into the inspected string. The appropriate number of modules to disconnect from string S<sub>M</sub> will depend on the orientation of string S<sub>P</sub> and on the irradiance conditions. It is important to note that our dEL procedure is able to eliminate ambient light for any irradiation level. However, the best configuration of the strings would be that at which string SP is oriented towards the sun -thus generating a high current- and where string S<sub>M</sub> is oriented in the opposite direction, such that the irradiation level on S<sub>M</sub> is low. In this way, the quality of the dEL images can be high, even using a limited number of on/off cycles [23]. In this way, the best configuration among those included in Fig. 6 would be the one corresponding to Fig. 6(d) which corresponds to the S<sub>M</sub> string facing east in the afternoon, and the strings Sp facing west. The best configurations are then when the dEL is carried out from the west (facing the sun) until the middle of the day, with the tracker facing west, and opposite in the central hours and in the afternoon. Camera positioning is manually optimized to prevent solar reflection artifacts from interfering with the imaging sensor, achieved through systematic adjustment of the camera-to-module angle.

Differences in the qualities of the dEL images in Fig. 6 are not clearly distinguishable due to the fact that the whole string was imaged –thus with a low-resolution image for the whole string. The quality of the dEL images is better when visualized on the individual pictures of the modules, see Fig. 7. It is important to note that the quality of the dEL images depends on different factors, such as the injected current, the aperture of the lens, the exposure time, the number of on/off cycles, etc. In any case, the visual quality of the different dEL images obtained was good enough to visualise the existing defects, as will be shown below. A more quantitative metric (such as the signal-to-noise ratio – SNR) will be addressed in future works.

The dEL images of the whole inspected string can be interesting since

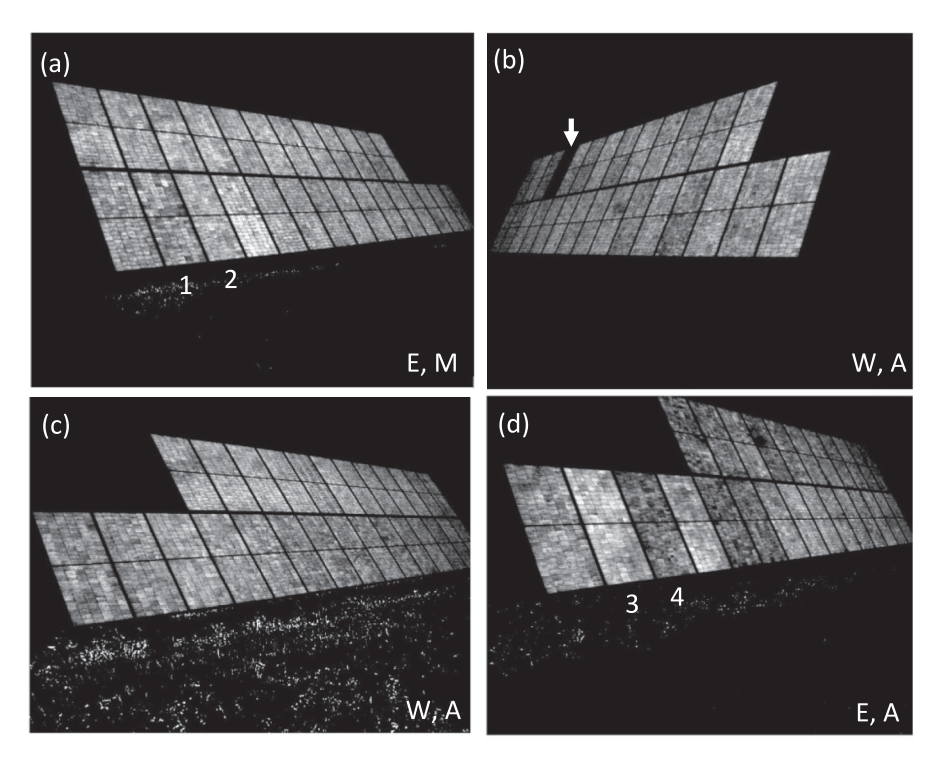


Fig. 6. Using the self-powering method, daylight EL (dEL) images of full strings for different configurations (E=east, W=west, M=morning, A=afternoon). Two modules were disconnected for (b), three for (a) and (c) and four for (d). (mc-Si monofacial half-cell technology).

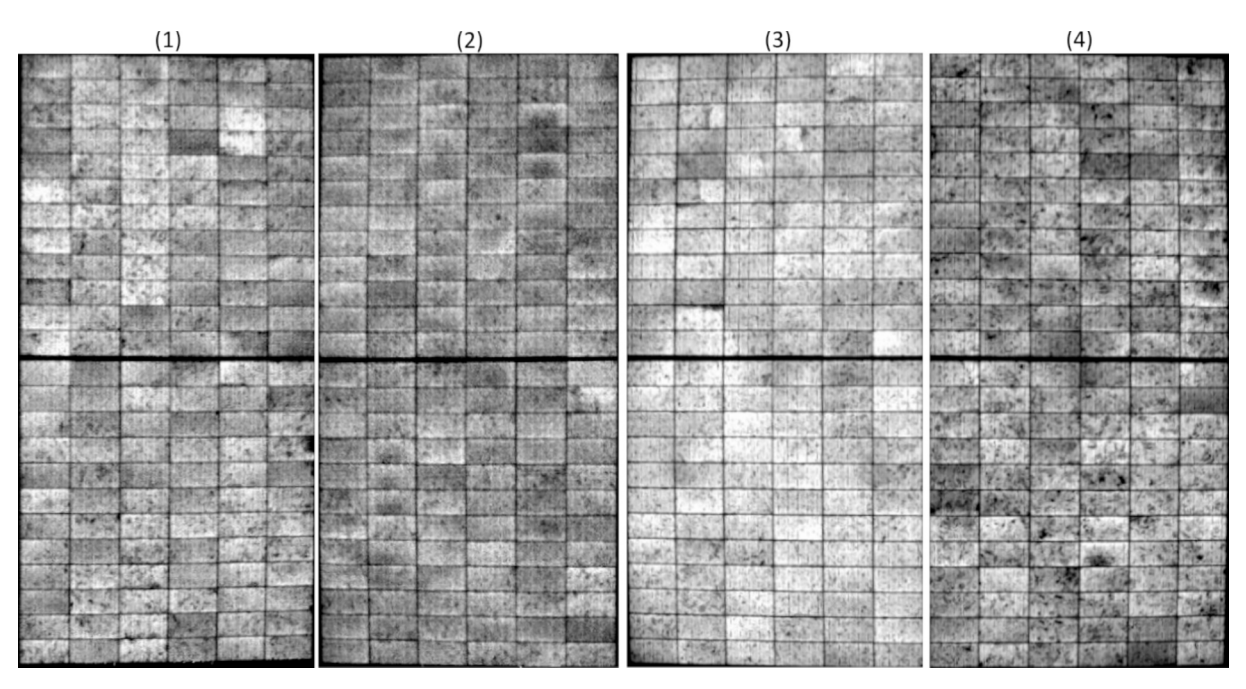


Fig. 7. Specific modules (marked in Fig. 6) inspected using the dEL self-powering method.

they allow major problems related to the modules to be distinguished. For instance, it is interesting to note that, as observed in Fig. 6(b), at the top left of the string, identified its position with an arrow, one of the modules of this string has been left accidentally disconnected from the rest of the strings, without this being noticed. This incident was successfully resolved with the help of dEL inspection of the whole string. In this case, the real number of disconnected modules from string  $S_M$  was really three rather than the initially intended two modules. On the other hand, the dEL images of the whole strings also allow major mismatches

between the modules to be distinguished (such as the case of the modules labelled #3 and #4 on Fig. 6(d)) or even between cells (such as the case of the module labelled #1 on Fig. 6 (a)).

4.2.2. Self-powering configuration for dEL images of individual modules Fig. 7 shows the dEL images of some individual modules, labelled as #1 and #2 (Fig. 6(a)) and #3 and #4 (Fig. 6(d)). To better utilise the sensor size of the InGaAs camera, each image taken is currently the image of two consecutive modules. In this way, it is possible to optimize

inspection times without compromising the resolution of the obtained dEL images. As can be seen, the quality of the images is sufficient to distinguish clear defects on the various solar cells. (Defect identification was visual and based on experience, and automated classification tools are planned for future work). This would be more clearly seen by comparing the dEL images with the lab-EL images obtained with a Si camera, as will be discussed later.

By comparing the dEL images of the individual modules, it is possible to observe a slightly better quality of the dEL images shown in Fig. 7 (1), (2), corresponding to those modules inspected with an optimum configuration, as discussed previously. In fact, while the injected current did not change greatly between the configurations used, the irradiation value was around  $300 \text{ W/m}^2$  in the case of the dEL images shown in Fig. 7 (3), (4), while it was around  $900 \text{ W/m}^2$  in the case of the dEL images shown in Fig. 7 (1), (2).

The dEL images of these individual modules also show that the module labelled #4 has a much lower general luminescence intensity emission than module #3 (Fig. 7 (3), (4)), which should be ascribed to the large number of solar cells that present defects in this module such as shunts or defects with the soldering (poor soldering). Large differences between the emission from the individual cells can also be seen, for example in module #1 (Fig. 7 (1)).

#### 4.2.3. Self-powering configuration for dEL images vs lab-EL images

In order to check the quality of our dEL images with reference to high-resolution EL images, some of the inspected modules were selected to make a detailed lab-EL inspection by disassembling the modules, sending them to a laboratory for lab-EL inspection with high resolution Si cameras (HR-lab-EL), and then sending them back to the plant and reassembling them in their original positions. Moreover, dEL inspections were performed both prior to disassembling the modules as well as after reassembly. Fig. 8 shows the comparison between the two images for two different modules, with lab-EL images obtained with a highresolution Si camera on the left side of each case, and the dEL image obtained by our self-powering configuration on the right side of each image. Additionally, Fig. 9 shows an enlarged view of some of the defects (marked with red boxes) shown in Fig. 8. The main defects on the different cells and metallic contacts are clearly visible in both cases –as highlighted in the images. In the case of our dEL images, some artificial brightness and contrasts are observed, which should be attributed to

artefacts of the lens used, and which is an area of improvement that we are already addressing.

The comparison of the dEL images against lab-EL images shows a significant difference in image quality (lower in the dEL), which originates from multiple technical factors: sensor resolution limitations, dual-module simultaneous imaging requirements, and field measurement complexities under high-irradiance operating conditions. Contributing factors include focusing optimization challenges, current stability issues related to meteorological variations such as cloud interference, and mechanical trackers displacement from wind-induced oscillations. These limiting parameters can be mitigated through systematic methodological improvements. Nonetheless, comparative assessment against lab-EL standards reveals acceptable diagnostic performance with effective defect detection capabilities.

### 4.2.4. Analysis of the observed defects by the dEL images with the self-powering configuration

Fig. 10 and Fig. 11 show other examples of dEL images with the self-powering configuration of individual modules obtained in the two inspected PV plants –thus with both c-Si and mc-Si technologies. The observed defects can be clustered into two large groups, one corresponding to defects with "high" electrical losses, and a second group in which losses are minimal, but which diminish overall plant performance over the years, and that may end up completely degrading the affected component [39,40].

The defects in the first group, which include blown fuses, open MC4 connectors, shorted modules, disconnected modules, broken modules (impacted or broken glass), deep cracks on the back of the module, etc., could be detected by other non-destructive analysis techniques such as thermography (manual or aerial), current analysis (in bus cable, CombinerBox input, DC inverter input, ...), IV curves, visual inspection, etc. However, if they can be performed quickly, such as in our proposed self-powering configuration, dEL inspections allow for much clearer identification. For example, Fig. 10(a) shows the dEL image of an inspected module in the mc-Si PV plant and reveals a large scratch along the backsheet on the top part of the inspected module. Fig. 10(a) shows also the thermography image taken very close to the module, where the defect can be also observed once it was detected by dEL inspection. Such a defect would go completely unnoticed in aerial thermography. Compared to its neighbouring cells, this scratch does not have a

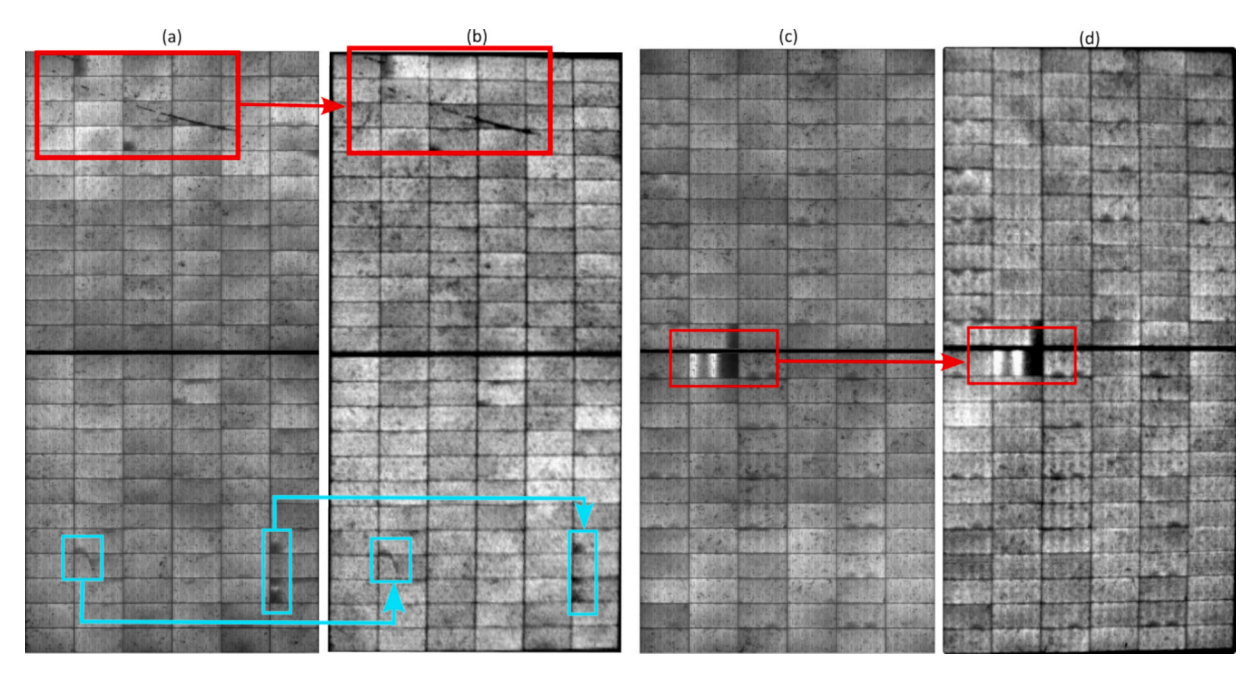
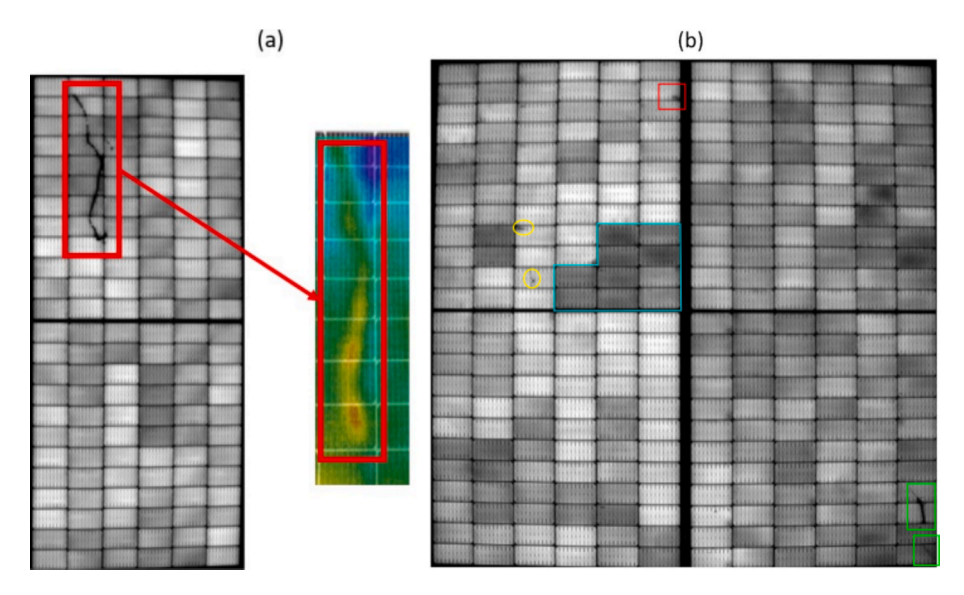


Fig. 8. (a) and (c) Black room standard test conditions lab-EL images. (b) and (d) Same two modules visualized through dEL in the self-powering configuration.

Fig. 9. Close-ups views of some of the defects observed in Fig. 8: (a) scratch, (b) broken solder joints to the central cross-connectors.



**Fig. 10.** Different types of defects detected in the inspected modules. (a) Large scratch on the top part of the module visualized through dEL imaging. The inset shows the thermography obtained with a manual camera of the upper part of the module, where the scratch is only "slightly" visible; (b) Various defects revealed through dEL imaging (green = scratch, blue = PID, yellow = shunt, red = inactive cell area). (For interpretation of the references to colour in this figure legend, the reader is referred to the web version of this article.)

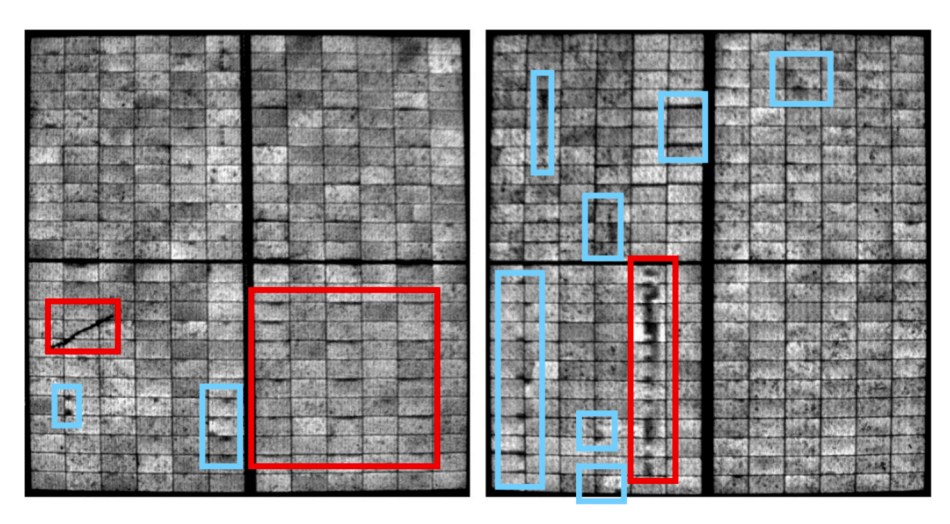


Fig. 11. Obtained dEL images of four modules, where different types of defects are detected.

temperature gradient (the maximum gradient within the red zone is  $3.2\,^{\circ}$ C) that would lead to it being considered a defect –as indicated by IEC 62446-3– such that it would have gone unnoticed and/or ruled out in thermography inspection. In contrast, by using the dEL it can clearly be seen that it is a major defect and that premature degradation can be averted –thus preventing subsequent energy/economic loss– by replacing the "damaged" module.

Defects in the second group would include mismatch, cracks in the rear part of the module, micro-breaks, slight impacts with partial damage to cell/s, cracks, multi-cracks, dendritic/tree-shape cracks or manufacturing defects in cells. These defects can only be detected by

overhead thermography or I-V characterization using big data techniques and pre-trained models. However, there is usually insufficient data available, such as inverter operating MPPT, which is often hidden by technologists as proprietary know-how. The advantage of the EL inspection technique is that it allows such defects to be clearly distinguished. Moreover, our dEL image by the self-powering configuration is able to distinguish it on-site. Fig. 10(b), for instance, shows the dEL images of two c-Si modules with different types of defects (green = scratch, blue=PID, yellow = shunt, red = inactive cell area). Fig. 11 shows additional dEL images of individual modules, where different types of defects detected in the inspected photovoltaic modules can be

seen, such as scratch, electrochemical corrosion and finger interruption, among others. Fig. 12 shows magnified views of the selected regions marked with red boxes in Fig. 11.

Potential damage caused by module disassembly, handling and reassembly has also been analysed. The results show that certain defects appeared in certain modules at some point during these processes. Fig. 13 presents one such case, where a scratch has been produced. Two EL images are shown in the figure: Fig. 13(a), taken with the InGaAs camera before disassembly; Fig. 13(b), taken with a Si camera after disassembly. Fig. 13(b) shows a defect that is not visible in Fig. 13(a) and which was not initially pinpointed. Fig. 13(c) and (d) show the area of this defect magnified for each image. The defect may thus be ascribed to the disassembly/handling process for High-Resolution nighttime EL (HR-lab-EL) inspection. This finding highlights the importance of using non-destructive inspection methods, such as on-site dEL imaging, to prevent damage to PV modules during EL inspection procedures.

This study validates a novel self-powered dEL inspection methodology that enables full-string PV module assessment in daylight without external power sources or module disassembly. The method significantly simplifies on-site EL imaging and provides operational advantages. Although our method is currently implemented manually, it allows for a full string inspection in under 5 min (including setup and image acquisition). Further automation, such as integration with trackers and drones, could bring throughput in line with that of current aerial inspections.

The main highlights of this work are:

- Operational simplicity: The configuration eliminates the need for generators, power supplies, or transport, enabling inspections under standard irradiance conditions using only plant infrastructure (eg. see Fig. 1 and Fig. 2).
- Cost-effectiveness: Reduced labour, equipment, and handling requirements lower O&M costs.
- **Non-invasiveness**: Avoiding disassembly minimizes risks of inducing secondary defects, as confirmed by comparative analysis with lab-EL images (eg. see Fig. 13).
- Comparable diagnostic quality: dEL images produced by this method clearly identify both critical and latent defects, even under variable irradiance, with good correlation to lab-EL standards (eg. see Fig. 8 and Fig. 9).
- **Field robustness**: The technique was successfully tested on more than 2,000 modules across varying irradiance and temperature conditions, demonstrating repeatability and adaptability.

- **Predictive potential**: It enables early identification of slow-degrading faults that are otherwise undetectable with conventional inspections like thermography or I–V analysis (eg. see Fig. 10).
- Deal with low illumination levels: As experimental validation confirms, the proposed method can deal at comparatively low illumination levels using several strings to power up the string under study.

In summary, this self-powered dEL methodology offers a scalable, cost-efficient, and reliable alternative for routine diagnostic inspections in large-scale PV plants. Despite moderate image quality characteristics, self-powered electroluminescence inspections provide significant operational benefits, including expedited inspection protocols and elimination of module removal procedures, while delivering comprehensive module performance assessment capabilities. Future work will focus on systematic methodological improvements, integrating automated defect classification and quantitative image metrics (e.g., SNR, contrast). Also, integrating this method with drone-mounted imaging systems could significantly improve the coverage and efficiency of PV module diagnostics, enabling rapid identification of electroluminescent signatures even under variable daylight conditions.

#### 5. Conclusions

Our work demonstrates that this non-invasive and rapid technique allows for effective defect detection, thereby maximizing energy production. This optimized method enables efficient electroluminescence inspections of photovoltaic modules in daylight, without requiring an external power source (such as a generator) or a stabilized current supply. This non-destructive analysis technique identifies defects that would otherwise prove challenging to detect.

The main advantages of this procedure are:

- No adjustable power supply is needed: the method eliminates the need for complex and costly external power sources.
- Reduced energy losses: modules remain in place during testing, thus avoiding energy losses and downtime associated with disassembly and reassembly.
- Lower costs and manpower requirements: staff and personnel hours and the need for specialized machinery and transportation equipment are significantly reduced.
- Minimized risk of damage: by avoiding repeated handling, the possibility of new or additional damage to modules is reduced.

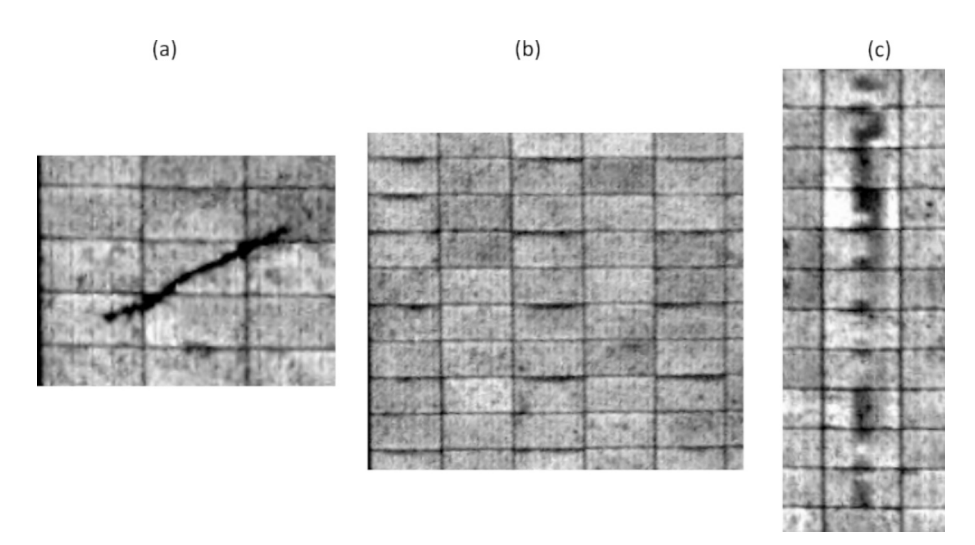


Fig. 12. Close-ups views of different defects observed in Fig. 11: (a) scratch, (b) electrochemical corrosion and (c) finger interruption.

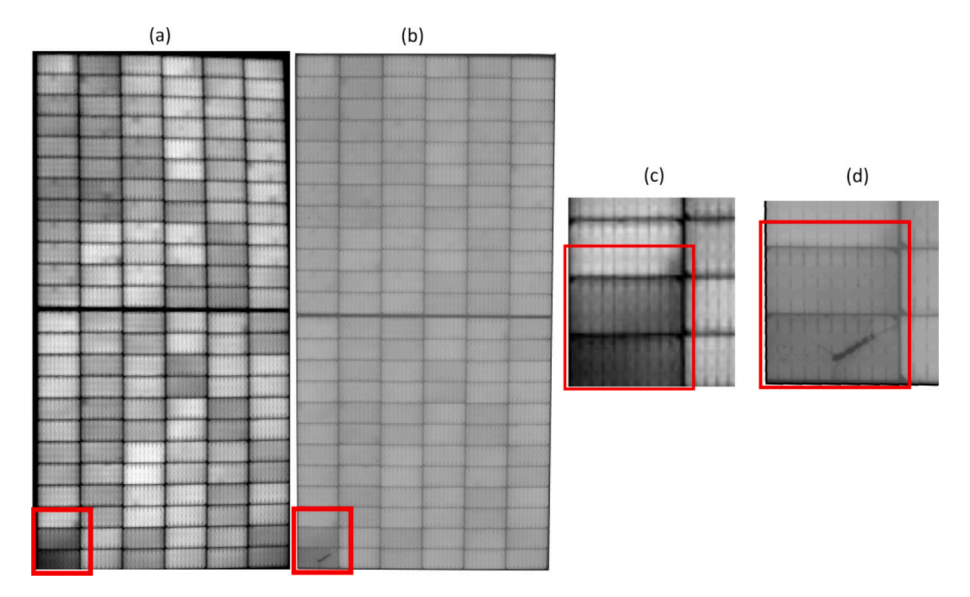


Fig. 13. (a) Pre-disassembly dEL image taken with the InGaAs camera; (b) HR-lab-EL taken with the Si camera after disassembling the module for darkroom inspection; (c) and (d) magnification of the region of interest.

- Daylight operation reduces risk and cost: inspections can be safely and efficiently conducted during daylight, eliminating the added complexity, risks, and costs of night-time work.
- Consistency with simulations: the developed simulations align closely with experimental results, thus validating the reliability and accuracy of this inspection method.

Overall, this approach offers a streamlined, sustainable, and costeffective solution for comprehensive PV module inspections.

#### CRediT authorship contribution statement

L.A. Carpintero: Writing – review & editing, Writing – original draft, Visualization, Methodology, Investigation, Formal analysis, Conceptualization. C. Terrados: Software, Methodology, Investigation. D. González-Francés: Visualization, Validation, Software, Methodology, Investigation. K.P. Sulca: Visualization, Validation, Software, Methodology, Investigation. V. Alonso: Writing – review & editing, Visualization, Validation, Supervision, Methodology, Investigation, Conceptualization. M.A. González: Visualization, Validation, Software, Methodology, Investigation. O. Martínez: Writing – review & editing, Writing – original draft, Supervision, Resources, Project administration, Conceptualization.

#### Declaration of competing interest

The authors declare that they have no known competing financial interests or personal relationships that could have appeared to influence the work reported in this paper.

#### Acknowledgments

This work has been financed by the Spanish Ministry of Science and Innovation, under projects PID2020-113533RB-C33 and PID2023-148369OB-C43, and by the Regional Government of Castilla y León (Junta de Castilla y León) and by the Ministry of Science and Innovation MICIN and the Spain (European Union) NextGenerationEU/PRTR ("Plan Complementario de Materiales Avanzados en Castilla y León"). K. Sulca has been funded under the call for predoctoral contracts UVa 2022, cofinanced by Banco Santander. C. Terrados is also grateful for the financial support received under project PDC2022-133419-I00, funded by MCIN/AEI/10.13039/ 501100011033 and NextGenerationEU/

#### PRTR.

#### References

- [1] Y. Krozer, Cost and benefit of renewable energy in the European Union, Renew. Energy 50 (2013) 68–73, https://doi.org/10.1016/j.renene.2012.06.014.
- [2] United Nations, Resolution A/RES/70/1. Transforming our world: the 2030 Agenda for Sustainable Development, 2015. https://docs.un.org/en/A/RES/70/1 (accessed February 14, 2025).
- [3] International Energy Agency, Renewables 2023 Analysis IEA, 2023. https://www.iea.org/reports/renewables-2023 (accessed February 14, 2025).
- [4] Z. Sun, X. Chen, Y. He, J. Li, J. Wang, H. Yan, Y. Zhang, Toward efficiency limits of crystalline silicon solar cells: recent progress in high-efficiency silicon heterojunction solar cells, Adv. Energy Mater. 12 (2022) 2200015, https://doi.org/ 10.1002/AENM.202200015.
- [5] B. Meban, World installed 600 GW of solar in 2024, could be installing 1 TW per year by 2030, https://www.Solarpowereurope.Org/Press-Releases/New-Report-World-Installed-600-Gw-of-Solar-in-2024-Could-Be-Installing-1-Tw-per-Year-by-2030 (2025)
- [6] IEC 62446-1. Photovoltaic (PV) systems: requirements for testing, documentation and maintenance. Part 1, Grid connected systems-documentation, commissioning tests and inspection, International Electrotechnical Commission, 2016.
- [7] M. Aghaei, A. Fairbrother, A. Gok, S. Ahmad, S. Kazim, K. Lobato, G. Oreski, A. Reinders, J. Schmitz, M. Theelen, P. Yilmaz, J. Kettle, Review of degradation and failure phenomena in photovoltaic modules, Renew. Sustain. Energy Rev. 159 (2022) 112160, https://doi.org/10.1016/J.RSER.2022.112160.
- [8] L. Koester, S. Lindig, A. Louwen, A. Astigarraga, G. Manzolini, D. Moser, Review of photovoltaic module degradation, field inspection techniques and technoeconomic assessment, Renew. Sustain. Energy Rev. 165 (2022) 112616, https:// doi.org/10.1016/J.RSER.2022.112616.
- [9] C. Del Pero, N. Aste, F. Leonforte, F. Sfolcini, Long-term reliability of photovoltaic c-Si modules – a detailed assessment based on the first Italian BIPV project, Solar Energy 264 (2023) 112074, https://doi.org/10.1016/J.SOLENER.2023.112074.
- [10] M. Waqar Akram, G. Li, Y. Jin, X. Chen, Failures of photovoltaic modules and their detection: a review, Appl. Energy 313 (2022) 118822, https://doi.org/10.1016/J. APENERGY 2022 118822
- [11] I. Høiaas, K. Grujic, A.G. Imenes, I. Burud, E. Olsen, N. Belbachir, Inspection and condition monitoring of large-scale photovoltaic power plants: a review of imaging technologies, Renew. Sustain. Energy Rev. 161 (2022) 112353, https://doi.org/ 10.1016/J.PSEP.2022.112352
- [12] M. Köntges, S. Kurtz, C. Packard, U. Jahn, K.A. Berger, K. Kato, T. Friesen, H. Liu, M. Van Iseghem, Report IEA-PVPS T13-01:2014. Review of Failures of Photovoltaic Modules Final, 2014. https://iea-pvps.org/key-topics/review-of-failures-of-photovoltaic-modules-final/ (accessed February 14, 2025).
- [13] International Electrotechnical Commission, IEC 60904-3:2019 Photovoltaic devices – Part 3: Measurement pr..., 2019. https://webstore.iec.ch/en/publicat ion/61084 (accessed February 14, 2025).
- [14] J. Coello, L. Pérez, F. Domínguez, M. Navarrete, On-site quality control of photovoltaic modules with the PV MOBILE LAB, in: Energy Procedia, Elsevier Ltd, 2014, pp. 89–98, https://doi.org/10.1016/j.egypro.2014.10.012.
- [15] J. Haunschild, M. Glatthaar, M. Demant, J. Nievendick, M. Motzko, S. Rein, E. R. Weber, Quality control of as-cut multicrystalline silicon wafers using photoluminescence imaging for solar cell production, Solar Energy Mater. Solar Cells 94 (2010) 2007–2012, https://doi.org/10.1016/j.solmat.2010.06.003.

- [16] B. Doll, J. Hepp, M. Hoffmann, R. Schuler, C. Buerhop-Lutz, I.M. Peters, J. A. Hauch, A. Maier, C.J. Brabec, Photoluminescence for defect detection on fullsized photovoltaic modules, IEEE J. Photovolt. 11 (2021) 1419–1429, https://doi. org/10.1109/JPHOTOV.2021.3099739.
- [17] H. Dreves, A Faster, Cheaper Way To Give Solar Panels a Clean Bill of Health, https://www.nrel.gov/news/detail/program/2023/a-faster-cheaper-way-to-give-solar-panels-a-clean-bill-of-health (2023).
- [18] G.A. dos Reis Benatto, C. Mantel, A.A. Santamaria Lancia, P.B. Poulsen, S. Forchhammer, S.V. Spataru, Laser induced luminescence characterization of mechanically stressed PV cells, in: 2021 IEEE 48th Photovoltaic Specialists Conference (PVSC), IEEE, 2021, pp. 1949–1953, https://doi.org/10.1109/ PVSC43889.2021.9518751.
- [19] High volume electroluminescence Analysis: AirBridgeOne, http://www.aepvi. com/ (n.d.).
- [20] Comprehensive Drone-Based Solar PV Inspection and Analysis, https://quantified-energy.com/ (n.d.).
- [21] J. Adams, B. Doll, C. Buerhop-Lutz, T. Pickel, J. Teubner, C. Camus, C.J. Brabec, Non-stationary outdoor EL-measurements with a fast and highly sensitive InGaAs camera, in: 32nd European Photovoltaic Solar Energy Conference and Exhibition (EU PVSEC 2016), 2016, pp. 1837–1841, https://doi.org/10.4229/ EUPVSEC20162016-5BV 1 15
- [22] G.A.D.R. Benatto, N. Riedel, S. Thorsteinsson, P.B. Poulsen, A. Thorseth, C. Dam-Hansen, C. Mantel, S. Forchhammer, K.H.B. Frederiksen, J. Vedde, M. Petersen, H. Voss, M. Messerschmidt, H. Parikh, S. Spataru, D. Sera, Development of outdoor luminescence imaging for drone-based PV array inspection, in: Proceedings of the IEEE International Conference on Computer Vision, Institute of Electrical and Electronics Engineers Inc, 2017, pp. 2682–2687, https://doi.org/10.1109/PVSC.2017.8366602.
- [23] M. Guada, Á. Moretón, S. Rodríguez-Conde, L.A. Sánchez, M. Martínez, M.Á. González, J. Jiménez, L. Pérez, V. Parra, O. Martínez, Daylight luminescence system for silicon solar panels based on a bias switching method, Energy Sci. Eng. 8 (2020) 3839–3853, https://doi.org/10.1002/ese3.781.
- [24] S. Koch, T. Weber, C. Sobottka, A. Fladung, P. Clemens, J. Berghold, Outdoor electroluminescence imaging of crystalline photovoltaic modules: comparative study between manual ground-level inspections and drone-based aerial surveys. Conference: European Photovoltaic Solar Energy Conference and ExhibitionAt: Munichvolume: 32nd, 2016.
- [25] L. Stoicescu, M. Reuter, J.H. Wener, Daysy: luminescence imaging of PV modules in daylight, n.d.
- [26] R. Bhoopathy, O. Kunz, M. Juhl, T. Trupke, Z. Hameiri, Outdoor photoluminescence imaging of photovoltaic modules with sunlight excitation, Prog. Photovoltaics: Res. Appl. 26 (2018) 69–73, https://doi.org/10.1002/ pin.2946.
- [27] O. Kunz, J. Schlipf, A. Fladung, Y.S. Khoo, K. Bedrich, T. Trupke, Z. Hameiri, Outdoor luminescence imaging of field-deployed PV modules, Prog. Energy 4 (2022) 042014. https://doi.org/10.1088/2516-1083/ac9a33.
- [28] W. Hermann, G. Eder, B. Farnung, G. Friesen, M. Köntges, B. Kubicek, O. Kunz, H. Liu, D. Parlevliet, I. Tsanakas, J. Vedde, Qualification of Photovoltaic (PV) Power Plants using Mobile Test Equipment 2021 PVPS Task 13 Performance, Operation and Reliability of Photovoltaic Systems, n.d. https://iea-pvps.org/research-tasks/performance-operation-and-reliability-of-pho-.

- [29] G.A.D.R. Benatto, R. Del Prado Santamaria, S.V. Spataru, M. Vuković, M. S. Marjavara, E. Olsen, I. Burud, Image quality evaluation of contactless outdoor photoluminescence based on string inverter's IV curve sweep capability, in: 40th European Photovoltaic Solar Energy Conference and Exhibition, 2023, https://doi.org/10.4229/EUPVSEC2023/4CV.1.19, 020383-001-005.
- [30] M. Vuković, M. Jakovljević, A.S. Flø, E. Olsen, I. Burud, Noninvasive photoluminescence imaging of silicon PV modules in daylight, Appl. Phys. Lett. 120 (2022), https://doi.org/10.1063/5.0097576.
- [31] J.W. Weber, O. Kunz, C. Knaack, D. Chung, A. Barson, A. Slade, Z. Ouyang, H. Gottlieb, T. Trupke, Daylight photoluminescence imaging of photovoltaic systems using inverter-based switching, Prog. Photovoltaics: Res. Appl. 32 (2024) 643–651, https://doi.org/10.1002/pip.3807.
- [32] M. Vuković, I. Eriksdatter Høiaas, M. Jakovljević, A. Svarstad Flø, E. Olsen, I. Burud, Photoluminescence imaging of silicon modules in a string, Prog. Photovoltaics: Res. Appl. 30 (2022) 436–446, https://doi.org/10.1002/pip.35.
- [33] L. Koester, A. Louwen, S. Lindig, G. Manzolini, D. Moser, Large-scale daylight photoluminescence: automated photovoltaic module operating point detection and performance loss assessment by quantitative signal analysis, Solar RRL 8 (2024), https://doi.org/10.1002/solr.202300676.
- [34] C. Terrados, D. González-Francés, J. Anaya, K.P. Sulca, V. Gómez-Alonso, M. A. González, O. Martínez, Improvements in the acquisition of daylight electroluminescence images using high speed cameras: comparison of square and sinusoidal waves excitations, in: 40th Eur. Photovolt. Sol. Energy Conf. Exhib., 2023, https://doi.org/10.4229/EUPVSEC2023/3DO.16.5, 3DO.16.5 (n.d.).
- [35] C. Terrados, D. González-Francés, K.P. Sulca, C. de Castro, M.A. González, O. Martínez, Towards contactless daylight photoluminescence of PV strings during operation by electrical modulation, Prog. Photovoltaics: Res. Appl. (2025), https://doi.org/10.1002/pip.70004.
- [36] C. Terrados, D. González-Frances, D. González-Fernández, V. Alonso, M.A. González, J. Jiménez, O. Martínez, Comparison of outdoor and indoor PL and EL images in Si solar cells and panels for defect detection and classification, J. Electron. Mater. 52 (n.d.) 5189–5198. https://doi.org/https://doi.org/10.1007/s11664-023-10535-2.
- [37] J.I. Morales-Aragonés, M.D.C. Alonso-García, S. Gallardo-Saavedra, V. Alonso-Gómez, J.L. Balenzategui, A. Redondo-Plaza, L. Hernández-Callejo, Online distributed measurement of dark I-V curves in photovoltaic plants, Appl. Sci. 11 (2021) 1924, https://doi.org/10.3390/APP11041924.
- [38] F.J. Toledo, J.M. Blanes, Geometric properties of the single-diode photovoltaic model and a new very simple method for parameters extraction, Renew. Energy 72 (2014) 125–133, https://doi.org/10.1016/j.renene.2014.06.032.
- [39] N. Saborido-Barba, C. García-López, J.A. Clavijo-Blanco, R. Jiménez-Castañeda, G. Álvarez-Tey, Methodology for calculating the damaged surface and its relationship with power loss in photovoltaic modules by electroluminescence inspection for corrective maintenance, Sensors 24 (2024) 1479, https://doi.org/ 10.3390/S24051479.
- [40] B. Jaeckel, M. Pander, P. Schenk, A. Linsenmeyer, J. Kirch, Nomenclature and description of Electro-Luminescence (EL) observations: cell cracks and other observations, EPJ Photovoltaics 15 (2024) 44, https://doi.org/10.1051/EPJPV/ 2024039.